Radio Science, Volume 36, Number 6, Pages 1723–1731, November/December 2001

Relationship between Jovian hectometric attenuation lanes and Io volcanic activity

J. D. Menietti and D. A. Gurnett

Department of Physics and Astronomy, University of Iowa, Iowa City, Iowa

J. R. Spencer and J. A. Stansberry

Lowell Observatory, Flagstaff, Arizona

Abstract. Within the Galileo plasma wave instrument data a narrow (in frequency) attenuation band is seen in the hectometric (HOM) emission that varies in frequency with system III longitude. This attenuation lane is believed to be the result of near-grazing incidence or coherent scattering of radio emission near the outer edge of the Io torus, i.e., when the ray path is nearly tangent to an L shell containing the Io flux tube [*Gurnett et al.*, 1998]. Such a process should, therefore, be enhanced when the Io volcanic activity is increased and the Io flux tube has enhanced density. We have performed a systematic study of the existing Galileo radio emission data in an effort to determine the phenomenology and frequency of occurrence of the attenuation lanes and the association, if any, with published volcanic activity of Io. Our results indicate that the attenuation lanes are present almost all of the time but are enhanced on occasion. The best examples of attenuation lanes occur when Galileo is within ~65 R_J of Jupiter and thus are probably more apparent because of the increased signal-to-noise ratio of the radio receivers. The lack of continuous monitoring of Io activity and the lack of known activity on the anti-Earthward side of Io are problematic and make detailed correlation with radio emission very difficult at this time. Nevertheless, if the data are displayed for periods when the spacecraft is within 65 R_J (i.e., for each perijove pass), then the highest-contrast lanes occur on most passes when the Io volcanic activity is also high for that pass. These results support our current understanding of attenuation lane formation and suggest that future efforts can be made to better understand the interaction of HOM emission with the Io flux tube.

1. Introduction

Jovian hectometric (HOM) radio emissions are generally described as emissions in the frequency range of ~200 kHz to ~3 MHz [cf. *Carr et al.*, 1983; *Ladreiter and Leblanc*, 1991]. Polarization measurements are consistent with a predominantly *X*-mode emission. The source mechanism is most likely the cyclotron maser instability, and the source region has been thought to be at L shells higher than L = 6.

Gurnett et al. [1998] have identified and explained a well-defined attenuation lane that becomes occasionally quite apparent in the HOM spectrograms and is modulated by the rotation of Jupiter. This attenuation lane occurs in the Jovian hectometric and lower frequency decametric radiation data from Galileo and is apparently the same feature as the "lanes" reported by *Green et al.* [1992] and *Higgins et al.* [1995, 1998] and the "drifting gap in the main late source" mentioned by *Lecacheux et al.* [1980]. In the Galileo data, as first reported by *Gurnett et al.* [1998], the center frequency varies systematically with the rotation of Jupiter and has two peaks per rotation (see Figure1). The attenuation band peaks in frequency near 50° central meridian longitude (CML) because of sources of HOM in the southern hemisphere, and it peaks near 185° because of sources in the northern hemisphere. It is believed that the attenuation occurs as the ray path from a high-latitude cyclotron maser source passes approximately parallel to the magnetic field near the northern or southern

Paper number 2000RS002458.
0048-6604/01/2000RS002458$11.00

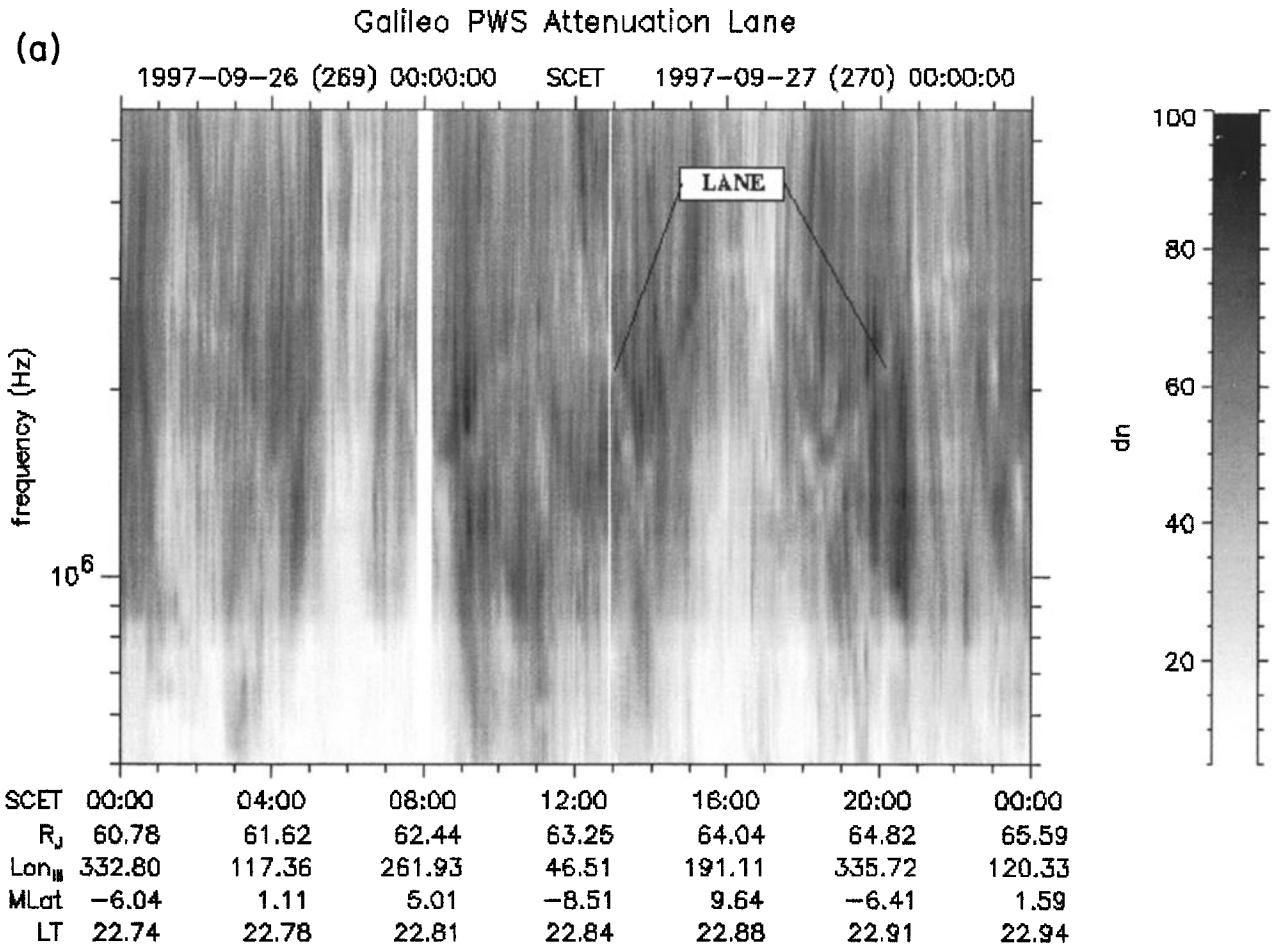

Figure 1. Frequency versus time spectrograms with wave intensity shown in gray scale. Each spectrogram shows an attenuation lane that varies in frequency as a function of system III longitude. Figure 1a is for day 269, 1997, and has been classified visibility index (VI) = 2.5, while Figure 1b is for day 260, 1997, and has been classified VI = 5.0. PWS, plasma wave receiver; SCET, spacecraft event time.

edges of an L shell containing the Io flux tube (IFT). Emission that is nearly tangent to this L shell may be scattered by density fluctuations or reflected at near-grazing incidence (see Figure 2 of *Gurnett et al.* [1998]). Thus this attenuation lane has aided in understanding the source location of the HOM emission. *Higgins et al.* (this issue) have also shown the effects of wave refraction near a sharp density gradient associated with the Io flux tube in producing the attenuation lanes.

Recently, *Menietti et al.* [1999] have shown that the mechanism for attenuating the radio emission is very efficient and a weak function of frequency. They showed examples of typical attenuation lanes with $I/I_o < 10^{-2}$, where I is the spectral density and I_o is the average spectral density near the lane edge. *Menietti et al.* [1999] showed that the attenuation lane is consistent with emission that is reflected at near-grazing incidence at the plasma boundary near the L shell containing the Io flux tube. This boundary forms a caustic surface that reflects the HOM emission in the range of frequencies 1-2 MHz. It was argued that the intermittent observation of the attenuation lane is related to the periodic increase in density of the IFT due to increased volcanic activity on Io.

Such a model is quite simple and assumes a sharp density gradient at the caustic surface. This assumption is not unreasonable assuming large periodic outflows of plasma along the IFT. We would expect that plasma flowing along the IFT would produce a sharp density gradient per-

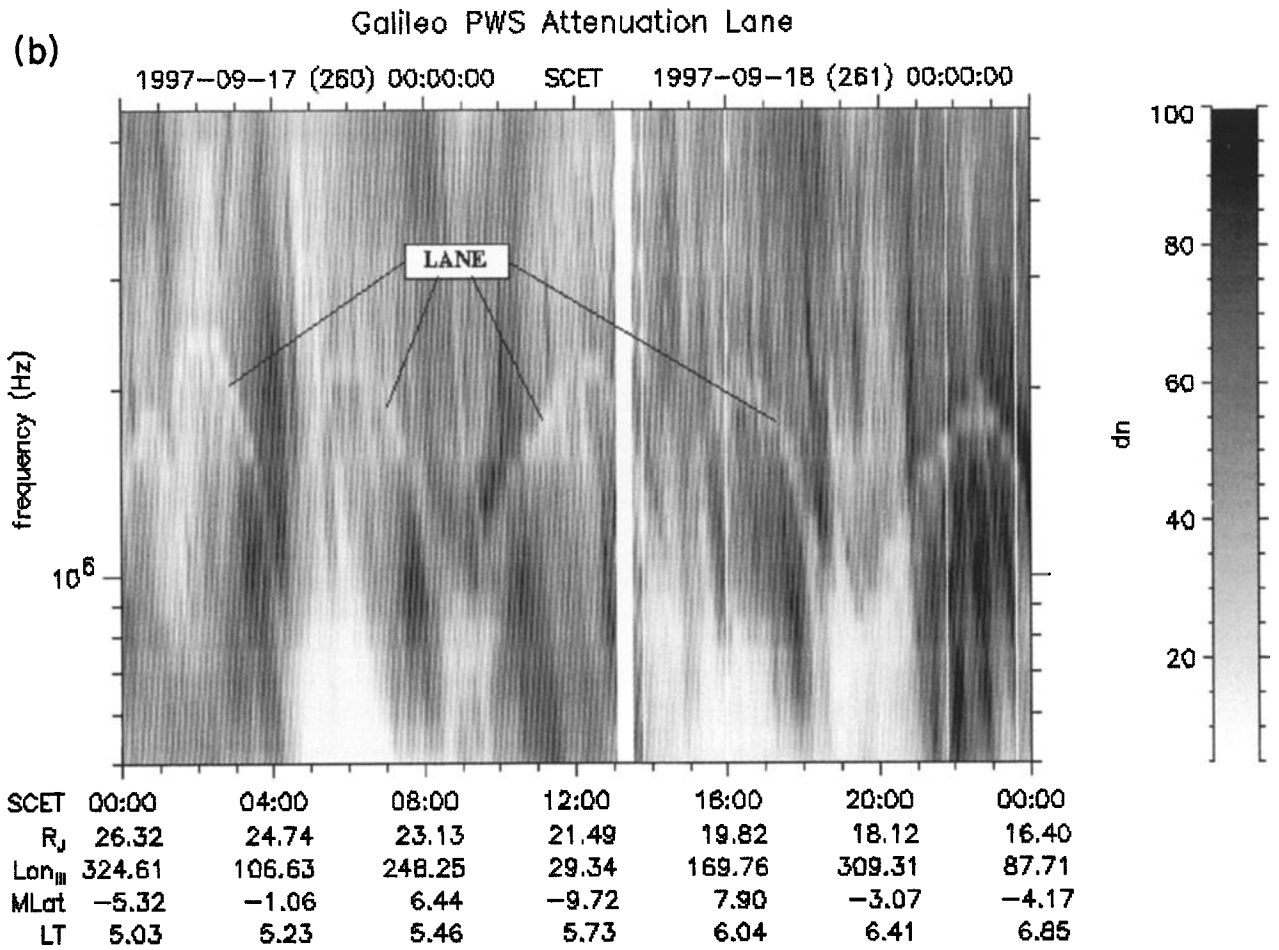

Figure 1. (continued)

pendicular to the magnetic field line within an ion gyroradius or so. Attenuation lanes should be more apparent, therefore, if Io volcanic activity levels are high and if the HOM emission levels are sufficient. In this paper we perform a statistical study of the phenomenology of the attenuation lanes seen by the Galileo plasma wave receiver (PWS) and examine possible correlations with Io volcanic activity levels. *Higgins et al.* [1999] have used a sorting technique to show that the attenuation lane is actually present as a dual-sinusoidal feature. In other words, the spacecraft often simultaneously observes attenuation from HOM sources in both the northern and southern Jovian hemispheres. However, the dominant attenuation lane occurs for sources in the same hemisphere as the spacecraft, and the attenuation lane resulting from emission in the opposite hemisphere is much fainter and typically not observable without special sorting techniques. In the study presented here, we consider only the dominant attenuation lane produced by HOM sources in the same Jovian hemisphere as the spacecraft.

2. Instrumentation

The plasma wave receiver on board Galileo consists of four different swept-frequency receivers that cover the frequency range from 5.6 Hz to 5.6 MHz for electric fields and 5.6 Hz to 160 kHz for magnetic fields. We will concentrate in this study on the electric fields obtained by the high-frequency receiver (HFR), which covers the frequency range from ~100 kHz to 5.6 MHz. A single electric dipole antenna with a tip-to-tip length of 6.6 m is connected to each electric receiver. A complete set of electric field measurements is obtained every 18.67 s with a frequency resolution of ~10% [cf. *Gurnett et al.*, 1992].

3. Observations and Analysis

To analyze the Galileo data, we individually examined frequency versus time spectrograms for the entire data set currently available. Each spectrogram spanned a 24-hour period and was displayed in black and white instead of color, because the attenuation lanes were usually most apparent in this contrast. A grading system was developed including 10 levels of clarity/contrast of the attenuation lanes determined by visual examination. We refer to this grading scale as a visibility index (VI). The visibility thus ranged from not visible through excellent visibility and contrast. Since the attenuation lane is a signature of the absence of emission, it is important to note that lanes are most conspicuous when they are dark in contrast to surrounding bright emission. Confusion can occur, therefore, when the HOM emission levels are particularly low. In this case the attenuation may have been clearly visible, but the HOM emission levels are too low for lanes to be seen in contrast. Each spectrogram, covering 1 full day, was classified with a visibility index (VI) number ranging from 0.5 to 5.0, with 0.5 corresponding to a very weak (or barely visible) lane, and 5.0 designating an exceptionally high contrast attenuation lane. For such a classification process, similar to classifying stellar types, there is undoubtedly human error. To diminish this error, the entire data set was independently analyzed twice at widely spaced times and compared to eliminate significant errors and discrepancies. The most outstanding examples of attenuation lanes are relatively easy to distinguish, however, and form a comparatively small subset of the data set. We have produced a data set of values of attenuation lane visibility index, with one numerical value for each day of the data. In Figure 1 we display spectrograms for 2 example days. Figure 1a shows an attenuation lane for day 269, 1997, that we have classified as VI = 2.5. Figure 1b depicts a spectrogram for day 260, 1997, with a higher contrast attenuation lane that we have classified as VI = 5.0.

In Figure 2 we display the visibility index (VI) versus time. The time is measured in running days, with day 1 being January 1 of the leap year 1996. Thus January 1, 1997, is running day 367, etc. This plot contains a total of 423 points, most of which lie at or below 2.0, which are considered weak contrast lanes. There are no data points in the following intervals of running days: days 317-347, 357-413, 423-443, 478-490, and 1001-1055. In the interval of days 680-931 there are only two data points with VI ≥ 3. These periods of no PWS data except for a few isolated days are shown with gray shading along the bottom of

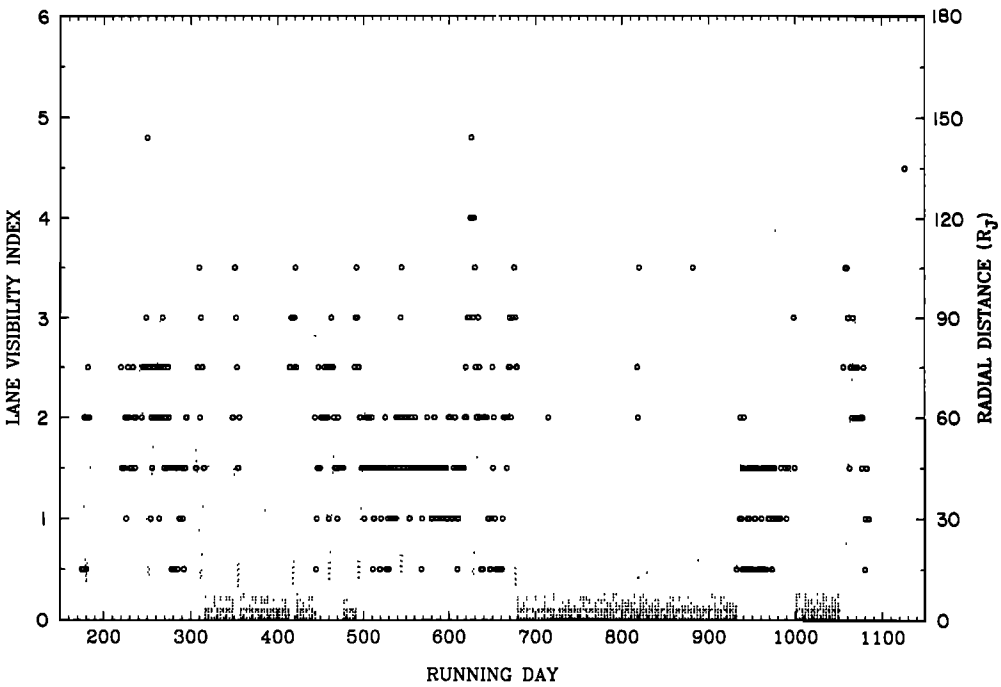

Figure 2. A plot of the attenuation lane visibility index (VI) versus time (circles). Each circle corresponds to one 24-hour period. The dotted curve depicts the spacecraft distance in units of R_J (on the right). The shaded regions indicate times when there was no data.

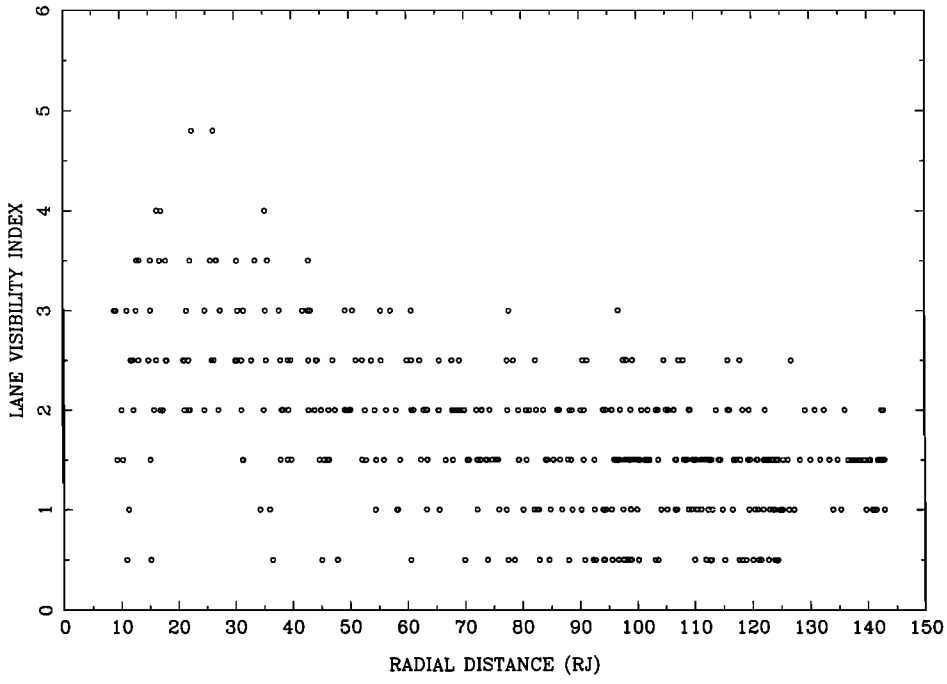

Figure 3. A plot of the visibility index versus radial distance of the spacecraft from Jupiter. There is a clear dependence on this parameter.

Figure 2. There is no discernable pattern on this plot, and attenuation lanes are observable on essentially all days with data. A faint attenuation lane was almost always visible at least at a level of VI = 0.5. The dotted curve depicts the spacecraft distance in units of R_J on the right side of the plot.

In Figure 3 we have plotted the visibility index as a function of spacecraft distance. Clearly, there is a correlation with radial distance. With the exception of only 2 days the highest levels of lane visibility all occurred for distances less than 65 R_J. While this could be a frequency-dependent beaming effect due to refraction, we believe it is the result of greater contrast of the lanes when the HOM emission levels are higher. The emission levels are all normalized to 100 R_J, but the ratio of signal to noise increases as the spacecraft is nearer to the source of HOM emission. Another necessary condition to observe an attenuation lane is a rather sharp plasma density gradient perpendicular to the Io flux tube. Since attenuation lanes are observed almost all of the time, but most clearly within ~65 R_J of Jupiter, we infer that a sharp density gradient perpendicular to the IFT and near its edge exists almost all of the time.

The volcanic activity level of Io has been monitored typically several times per month for a number of years [cf. *Spencer et al.*, 1997]. The data were taken using the NASA Infrared Telescope Facility (IRTF) on Mauna Kea, with the NSFCAM 1-5-μm infrared camera, and the Perkins 72" telescope at Lowell Observatory, with the Ohio State Infrared Imager/Spectrometer (OSIRIS) 1-2.5-μm camera. Other related studies at lower temperatures (5-20 μm) are reported by *Blaney et al.* [1997] and *Veeder et al.* [1994]. We present here a more comprehensive list of quantitative infrared brightness measurements made over five different wavelengths (λ = 1.7, 2.3, 3.5, 3.8, and 4.8 μm) over a period of time including the Galileo mission. The field of view of the observations is effectively the entire hemisphere of Io at the wavelengths observed. In a general sense the infrared observations made at longer wavelengths are dominated by cooler lava flows while those at shorter wavelengths are of the hottest, most vigorous lava flows and surface hot spots. We have chosen to use 2.3- and 3.5-μm data, because these wavelengths are more frequently monitored and indicate the hotter sources. In particular, we have used the 3.5-μm data when available. If they were not available, we used the 2.3-μm data after converting the latter to an equivalent 3.5-μm flux using a typical 2.3/3.5-μm color temperature of 650 K [*Spencer et al.*, 1997]. This gives a 3.5/2.27-μm flux ratio of 3.55. In Figure 4 we display a plot (diamonds connected by dotted line) of these brightnesses (GW/μm/sr) as a function of running day. This plot indicates two general regions of high volcanic activity: the

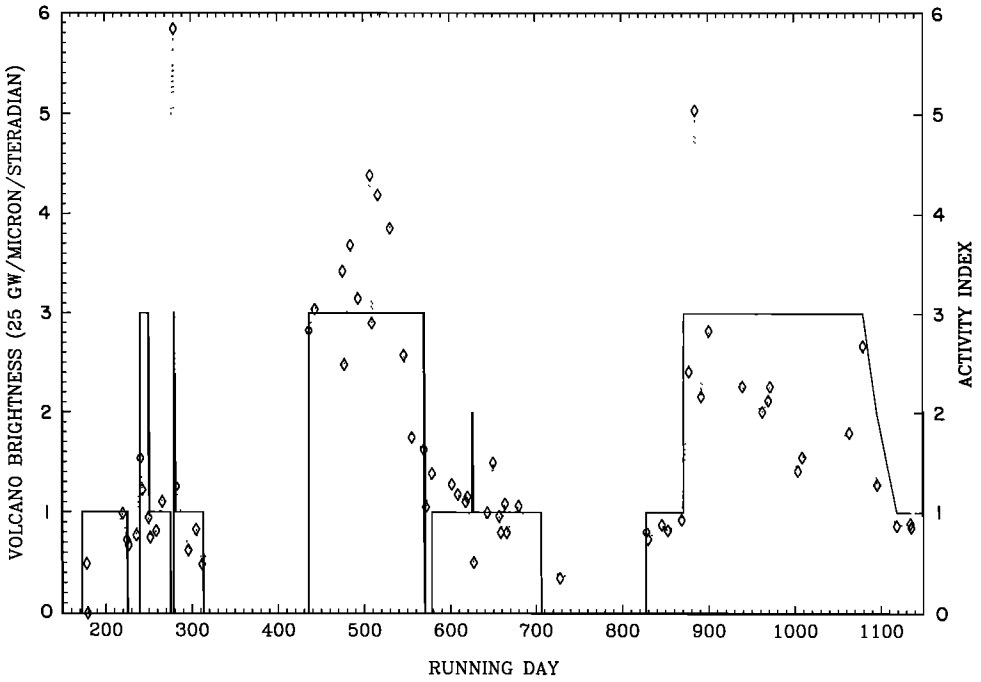

Figure 4. A plot of the volcanic activity brightness (25 GW/μm/sr) versus time for a number of observations made at Lowell Observatory and Mauna Kea (diamonds). Superimposed on this plot (solid line) is the volcanic activity index as defined in the text (right vertical axis).

period from about day 440 to about day 570 and the period from about day 880 to day 1100. Exceptionally high activity was reported on days 280, 524, and 885. Periods of more modest activity lie in the time ranges from days 240 to 250 and days 580 to 680. Elsewhere the brightness is reported as low.

An informal and qualitative record of volcanic activity is also maintained at the Jupiter Watch Web site (available from the Lowell Observatory at http://www.lowell.edu/users/ijw/volnews.html). The Jupiter Watch Web site includes qualitative information pertaining to ground-based and Hubble Space Telescope observations in the approximate wavelength range for 1 to 5 μm. Additional comments from the Galileo Solid State Imager team and the Near-Infrared Mapping Spectrometer experiment observation team are included as well. Even though this information is not quantitative, it is invaluable for establishing a time line of volcanic activity. It is difficult to assign a quantitative index to the volcanic activity, because it is unknown what quantity of material is actually dispersed into the magnetosphere with each known eruption. For this reason, we have only used three levels: Level 0 for periods with no reported observations, level 1 for observed low or normal activity levels, and level 3 for observed periods of large volcanic activity. Level 2 was a special designation for one event discussed below. We emphasize that the volcanic activity index (AI) is only a crude index of the presence of known volcanic activity on the side of Io facing the observer. It is not an indication of the size or volume of ejecta of the volcanoes, as it is unclear how much ejecta actually reaches the torus as plasma. In addition, there are many gaps in the monitoring of volcanic activity. Even periods that are designated as monitored are most likely not continuously but only periodically observed. In Figure 4 the volcanic activity index (solid line, right-hand scale) is shown plotted as a function of running day. The Jupiter Watch Web site information has been used in addition to the data of Figure 3 to define the index for each day. For day 626 we have recorded AI = 2, rather than 3, because the comments for observations indicated strong evidence for very recent volcanic activity on or near this day.

The next step in the analysis was to use the information provided by Figure 3. From this plot we note that only two values of VI ≥ 3 occur for spacecraft radial distances r greater than 65 R_J because of signal-to-noise capabilities of the PWS HFR. These days were in 1996: days 266 ($r \sim 90\ R_J$) and 268 ($r \sim 95\ R_J$). Consequently, in Figure 5 we

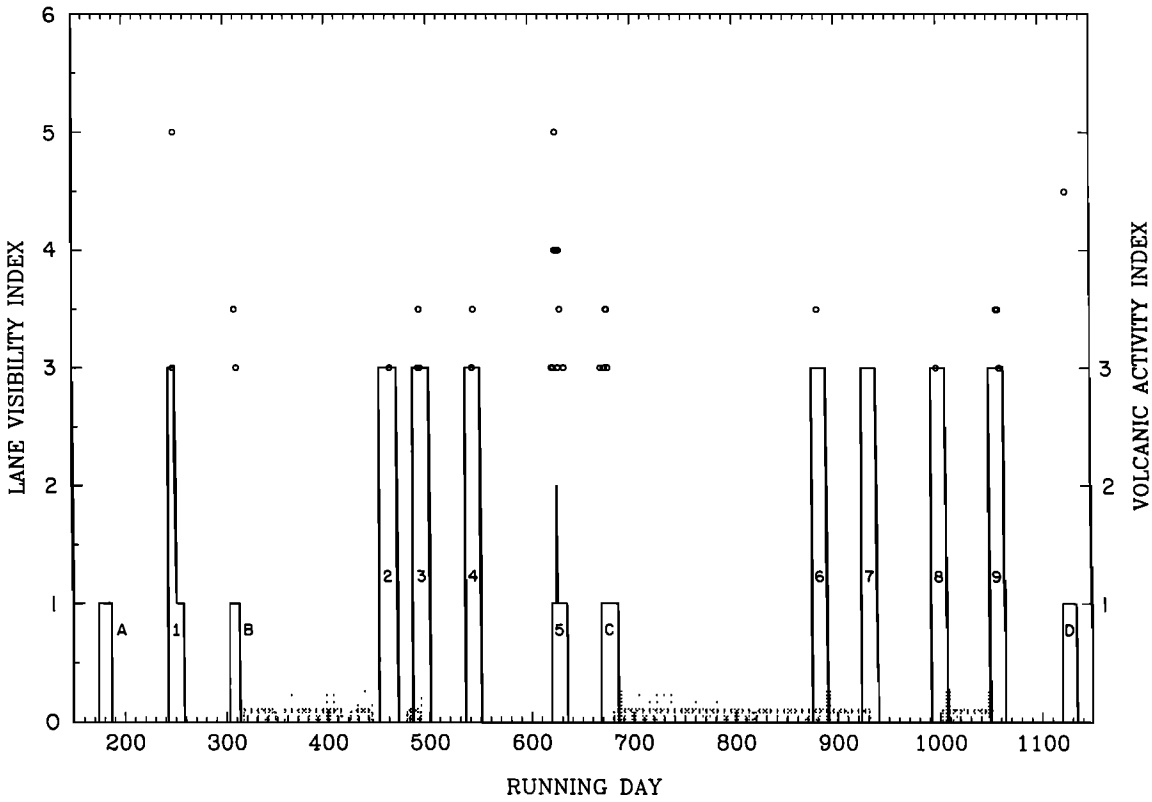

Figure 5. A plot of values of VI ≥ 3 which occur for AI ≠ 0. Both VI and AI are plotted only for times when the spacecraft radial distance was less than 65 R_J. A possible relationship between the two indices is indicated. The numbered events depict nine episodes of AI ≥ 2. The lettered episodes, A, B, C, and D, have AI = 1.

plot only those values of VI ≥ 3 which occur for AI ≠ 0, and only when the spacecraft distance was less than 65 R_J. With these constraints a possible relationship between VI and AI emerges. Nine episodes of AI ≥ 2 occur as numbered on the plot. Each of these nine episodes contains less than 20 days and occurs during a single perijove pass. For eight of the nine episodes there is at least 1 day when VI ≥ 3. Episode 7 is the only exception, but only during half of episode 7 were data available from PWS. Table 1 indicates the number of days of each episode N_e, the number of days of PWS data during the episode N_t, and the number of days during the episode with VI ≥ 3, N_I. There are also four lettered episodes (episodes A, B, C, and D) with reported volcanic activity at low or normal levels, i.e., AI = 1. For three of these episodes (episodes B, C, and D) there are 1 or more days with VI ≥ 3. These three episodes and episode 7 are therefore anomalous in that VI and AI are in contrast. On only 2 of the 13 perijove passes (episodes A and 7) was VI < 3.

Table 1. Statistics of the Episodes of Figure 5

Episode	1	2	3	4	5	6	7	8	9
N_e	7	18	17	15.5	1	15	15	15	15.5
N_t	7	18	17	15.5	1	1	5	1	8
N_I	2	1	3	2	1	1	0	1	5

4. Summary and Conclusions

We have conducted a survey of all the Galileo radio wave data through January 31, 1999. The results indicate that attenuation lanes resulting from scattering of radio waves that are nearly tangent to an L shell that is close to the Io flux tube occur almost all the time. Such lanes, however, are much more evident when the spacecraft is within ~65 R_J of Jupiter. By plotting attenuation lane visibility index and the index of known volcanic activity versus time we find that there is a possible relationship if the data are constrained to spacecraft distances of $r \leq 65\ R_J$.

At least two conditions are necessary for the attenuation lanes to appear in strong contrast to the HOM emission.

First, the broadband power spectral energy density of the HOM must be high, and second, the plasma density along the IFT should be relatively high compared to the Jovian magnetospheric density. Apparently, this latter condition is true most of the time, because the attenuation lanes are observable almost all of the time. There is no published record of Io plasma torus density at the present time. The lanes reach their highest visibility most frequently when the spacecraft radial distance $r \lesssim 65\ R_J$ (Figure 3). This is the case probably because the spacecraft plasma wave receivers are most sensitive to the HOM emission levels when the spacecraft is close to the source region, and the attenuation lanes are more clearly observed in contrast to the emission. However, near day 268 of 1996 the attenuation lanes were particularly visible (VI = 3.0) when $r > 90\ R_J$. Since the AI for this day is only 1, this suggests a particularly strong volcanic event that was not recorded.

During periods of high density along the IFT a strong density gradient perpendicular to the magnetic field exists near the point of tangency of the HOM emission. Under these conditions we expect efficient reflection of HOM emission over a narrow bandwidth [cf. *Menietti et al.*, 1999]. It is also possible that higher than normal densities along an L shell near the IFT would increase the efficiency of coherent scattering of HOM emission near the point of tangency of the emission with the magnetic field. It is possible that increased volcanic activity occurred on the side of Io not facing the observer or that activity occurred during gaps in the observations. Many of the events recorded in *Spencer et al.* [1997] or on the Jupiter Watch Web site took many days and weeks to develop to maximum infrared output, and the actual time between eruption and the filling of the IFT is not known. *Spencer et al.* [1994] note, for instance, that Loki, Io's most powerful single volcano, undergoes periodic brightenings of several months duration. However, many events are known to be short duration (only a day or two); thus many events will be missed by noncontinuous observations. Variable attenuation lane visibility observed on time scales less than 24 hours indicates possible inhomogeneous plasma distribution along the Io flux tube and/or temporal effects of Io volcanic activity. Modeling of flux tube filling will be important for better understanding of the observations. Another difficulty cited by *Spencer et al.* [1997] is that even intense infrared activity is not always accompanied by plumes or visible surface changes (eruption). Thus there are many reasons to expect a less than perfect correlation between the volcanic activity index and the attenuation lane visibility index.

A number of conclusions are possible resulting from our study of the phenomenology of the attenuation lanes. Attenuation lanes are visible on almost every day of Galileo observations, but appear strongest for radial distances of $<65\ R_J$. The association shown in Figure 5 is consistent with the current understanding of the formation of the attenuation lanes even if a detailed correlation is not possible. This implies that a relatively strong density gradient perpendicular to the Io flux tube exists almost all of the time, but particularly when Io volcanic activity increases. It is hoped that more comprehensive monitoring of Io volcanic activity in the future will aid in better understanding the interaction of HOM emission with the Io flux tube.

Acknowledgments. We wish to thank Nick Schneider, Jody Wilson, and Rosaly Lopes-Gautier for excellent discussions concerning this work. We thank J. Hospodarsky for typesetting this manuscript and J. B. Groene and T. F. Averkamp for assistance with graphical software. This analysis was supported by NASA through contract 958779 with the Jet Propulsion Laboratory and by NASA grant NAG5-8918.

References

Blaney, D. L., G. J. Veeder, D. L. Matson, T. V. Johnson, J. D. Goguen, and J. R. Spencer, Io's thermal anomalies: Clues to their origins from comparison of ground-based observations between 1 and 20 μm, *Geophys. Res. Lett.*, *24*, 2459-2462, 1997.

Carr, T. D., M. D. Desch, and J. K. Alexander, Phenomenology of magnetospheric radio emissions, in *Physics of the Jovian Magnetosphere*, edited by A. J. Dessler, pp. 226-284, Cambridge Univ. Press, New York, 1983.

Green, J. L., J. R. Thieman, C. Higgins, S. F. Fung, R. M. Candey, and L. Aist-Sagara, Lane features in Jovian hectometric radio emissions, in *Physics of the Jovian Magnetosphere*, edited by H. O. Rucker, S. J. Bauer, and M. L. Kaiser, pp. 91-103, Austrian Acad. of Sci., Vienna, 1992.

Gurnett, D. A., W. S. Kurth, R. R. Shaw, A. Roux, R. Gendrin, C. F. Kennel, F. L. Scarf, and S. D. Shawhan, The Galileo plasma wave investigation, *Space Sci. Rev.*, *60*, 341-355, 1992.

Gurnett, D. A., W. S. Kurth, J. D. Menietti, and A. M. Persoon, An unusual rotationally modulated attenuation band in the Jovian hectometric radio emission spectrum, *Geophys. Res. Lett.*, *25*, 1841-1844, 1998.

Higgins, C. A., J. L. Green, J. R. Thieman, S. F. Fung, and R. M. Candey, Structure within Jovian hectometric radiation, *J. Geophys. Res.*, *100*, 19,487-19,496, 1995.

Higgins, C. A., J. R. Thieman, S. F. Fung, J. L. Green, and R. M. Candey, Latitudinal structure within Jovian hectometric radiation, *J. Geophys. Res.*, *103*, 26,679-26,686, 1998.

Higgins, C. A, J. R. Thieman, S. F. Fung, J. L. Green, and R. M. Candey, Jovian dual-sinusoidal HOM lane features observed by Galileo, *Geophys. Res. Lett.*, *26*, 389-392, 1999.

Higgins, C. A., J. R. Thieman, S. F. Fung, J. L. Green, and R. M. Candey, Simple ray tracing of Galileo-observed hectometric attenuation features, *Radio Sci.*, this issue.

Ladreiter, H. P., and Y. Leblanc, The Jovian hectometric radiation: An overview after the Voyager mission, *Ann. Geophys.*, *9*, 784-796, 1991.

Lecacheux, A., B. Boller-Pedersen, A. C. Riddle, J. B. Pearce, A. Boischot, and J. W. Warwick, Some special characteristics of the hectometric Jovian emission, *J. Geophys. Res.*, *85*, 6877-6882, 1980.

Menietti, J. D., D. A. Gurnett, W. S. Kurth, and J. B. Groene, Effectiveness of near-grazing incidence reflection in creating the rotationally modulated lanes in the Jovian hectometric radio emission spectrum, *Radio Sci.*, *34*, 1005-1012, 1999.

Spencer, J. R., B. E. Clark, L. M. Woodney, W. M. Sinton, and D. Toomey, Io hot spots in 1991: Results from Europa occulation photometry and infrared imaging, *Icarus*, *107*, 195-208, 1994.

Spencer, J. R., J. A. Stansberry, C. Dumas, D. Vakil, R. Pregler, M. Hicks, and K. Hege, A history of high-temperature Io volcanism: February 1995 to May 1997, *Geophys. Res. Lett.*, *24*, 2451-2454, 1997.

Veeder, G. J., D. L. Matson, T. V. Johnson, D. L. Blaney, and J. D. Goguen, Io's heat flow from infrared radiometry: 1983-1993, *J. Geophys. Res.*, *99*, 17,095-17,162,1994.

D. A. Gurnett, J. D. Menietti, Department of Physics and Astronomy, University of Iowa, Iowa City, IA 52242-1479. (donald-gurnett@uiowa.edu; jdm@space.physics.uiowa.edu)

J. R. Spencer and J. A. Stansberry, Lowell Observatory, 1400 West Mars Hill Road, Flagstaff, AZ 86001. (spencer@lowell.edu; stansber@as.arizona.edu)

(Received May 14, 2000; revised August 9, 2000; accepted August 16, 2000.)